GREENER GRASS: ENHANCING GNNS WITH ENCODING, REWIRING, AND ATTENTION

Anonymous authors
Paper under double-blind review

ABSTRACT

Graph Neural Networks (GNNs) have become important tools for machine learning on graph-structured data. In this paper, we explore the synergistic combination of graph encoding, graph rewiring, and graph attention, by introducing Graph Attention with Stochastic Structures (GRASS), a novel GNN architecture. GRASS utilizes relative random walk probabilities (RRWP) encoding and a novel decomposed variant (D-RRWP) to efficiently capture structural information. It rewires the input graph by superimposing a random regular graph to enhance long-range information propagation. It also employs a novel additive attention mechanism tailored for graph-structured data. Our empirical evaluations demonstrate that GRASS achieves state-of-the-art performance on multiple benchmark datasets, including a 20.3% improvement in ZINC MAE.

1 INTRODUCTION

Graph Neural Networks (GNNs) have revolutionized machine learning tasks involving graph-structured data (Wu et al., 2020; Veličković, 2023). Various paradigms within GNNs offer distinct advantages: message-passing neural networks (MPNNs) effectively leverage local graph structure (Kipf and Welling, 2016) and are often complemented with graph rewiring techniques to modify the graph's topology and facilitate message passing (Topping et al., 2021); Graph Transformers (GTs) incorporate attention mechanisms to capture global dependencies (Yun et al., 2019; Rampášek et al., 2022) and can be enhanced by graph encoding methods that enrich node and edge features with structural information (Dwivedi et al., 2021; 2023).

The goal of our paper is to create a new architecture that can possess the advantageous properties of the above listed methods. To achieve our goal, we propose Graph Attention with Stochastic Structures (GRASS), a GNN architecture that synergistically combines random walk encoding, random rewiring, and also *introduces a new additive attention mechanism* designed for graph-structured data. We demonstrate that the combination of these components can lead to improved performance on a wide range of graph-structured learning tasks.

To this end, we conduct a series of experiments on multiple benchmark datasets and perform various ablation studies to assess the performance of GRASS. Our results show that GRASS achieves competitive or superior performance compared to existing methods on multiple popular datasets, suggesting that the synergy of graph encoding, random rewiring, and attention mechanism can effectively enhance GNNs.

Our Contributions.

- We propose GRASS, a GNN architecture that integrates random walk encoding, random rewiring, and a novel additive attention mechanism designed for graphs.
- We analyze these components with respect to desirable properties of a GNN and provide insights into how they contribute to the model's performance.
- We provide empirical evidence through experiments and ablation studies that a carefully selected combination of these components can lead to improved performance on multiple benchmark datasets.

In the remainder of the paper, we review related work in Section 2, describe the architecture of GRASS in Section 3, present experimental results in Section 4, and draw conclusions in Section 5.

2 Related Work

In this section, we summarize some of the previous work related to the main concepts of GRASS.

Message-Passing Neural Networks. Message-Passing Neural Networks (MPNNs), such as Graph Convolutional Networks (GCNs) (Kipf and Welling, 2016), GraphSAGE (Hamilton et al., 2017), and Graph Isomorphism Networks (GIN) (Xu et al., 2018), propagate information within local neighborhoods of a graph. By aligning computation with the structure of the graph, MPNNs offer a strong inductive bias for graph-structured data (Ma et al., 2023).

Graph Rewiring. Graph rewiring techniques modify the topology of the graphs to improve their connectivity, often leveraging spectral properties to guide the process (Topping et al., 2021; Arnaiz-Rodriguez et al., 2022). Rewiring improves MPNNs by alleviating issues in information propagation, such as underreaching, which occurs when distant nodes cannot communicate (Alon and Yahav, 2020). In this work, we explore a form of random rewiring that superimposes a random regular graph on the input graph.

Graph Transformers. Attention mechanisms (Vaswani et al., 2017) allow GNNs to weigh the importance of neighboring nodes during aggregation (Veličković et al., 2017). Graph Transformers (GTs), such as Graph Transformer Network (GTN) (Yun et al., 2019), extend this idea to global attention across nodes. GTs often inherit attention mechanisms designed for sequences, which may not be optimal for graphs (Chen et al., 2024). Designing attention mechanisms specifically for graph-structured data is an active area of research, and we aim to contribute to it by proposing a novel additive attention mechanism.

Graph Encoding. Enhancing node and edge features with graph encodings has been shown to improve GNN performance (Dwivedi et al., 2023). Techniques such as Laplacian positional encodings (LapPE) (Dwivedi et al., 2021) and relative random walk probabilities (RRWP) encoding (Ma et al., 2023) incorporate structural information into node and edge features, enhancing GTs, which otherwise lack a graph inductive bias (Ma et al., 2023). We utilize RRWP encoding in GRASS, and propose a decomposed variant (D-RRWP) with improved computational efficiency.

Notable Combinations. The General, Powerful, Scalable (GPS) Graph Transformer (Rampášek et al., 2022) represents a hybrid of MPNN and GT, merging the inductive bias of message passing with the global perspective of Transformers. Exphormer (Shirzad et al., 2023) combines GTs and rewiring by adding random edges and supernodes, generalizing BigBird (Zaheer et al., 2020), a sparse Transformer, to graph-structured data.

Our work builds upon these paradigms by incorporating random walk encoding and random rewiring, and we also create a novel additive attention mechanism tailored for graphs. Although RRWP encoding and random rewiring have been explored separately (Ma et al., 2023; Shirzad et al., 2023), their combination with each other and a graph-tailored attention mechanism is, to the best of our knowledge, novel. Our experiments show that this architecture not only matches but often exceeds state-of-the-art performance across a wide range of benchmark problems.

3 Methods

In this section, we introduce the design of GRASS. We begin by examining the desirable qualities of a GNN, which guide our architectural design. Subsequently, we introduce the components of GRASS by following the order of data processing in our model, and describe the role of each component in terms of the design goals.

Design Goals. We center our design around what we consider to be the key characteristics of an effective GNN. We will focus on the processing of nodes (*N1–N3*) and edges (*E1–E2*) of the model.

N1. *Permutation Equivariance.* Unlike tokens in a sentence or pixels in an image, nodes in a graph are unordered, and therefore the model should be permutation equivariant by construction. Since reordering the nodes of a graph does not change the graph, permuting the nodes of the

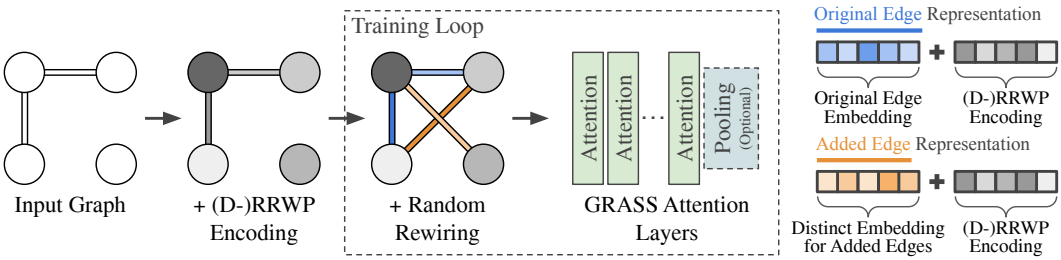

Figure 1: The high-level structure of GRASS. GRASS precomputes (D-)RRWP encodings. At each training iteration, it rewires the input graph and adds distinct embeddings to added edges.

input graph of a GNN layer should only result in the same permutation of its output (Veličković, 2023). Formally, let $f(\mathbf{X}, \mathbf{E}, \mathbf{A})$ be the function computed by a layer, where $\mathbf{X} : \mathbb{R}^{|V| \times n_{\text{node}}}$ represents node features with n_{node} dimensions, $\mathbf{E} : \mathbb{R}^{|V| \times |V| \times n_{\text{edge}}}$ represents edge features with n_{edge} dimensions, and $\mathbf{A} : \{0,1\}^{|V| \times |V|}$ represents the adjacency matrix (edge weights are considered scalar-valued edge features). If the layer is permutation equivariant and $(\mathbf{X}_{\text{out}}, \mathbf{E}_{\text{out}}) = f(\mathbf{X}_{\text{in}}, \mathbf{E}_{\text{in}}, \mathbf{A})$, then $(\mathbf{P}\mathbf{X}_{\text{out}}, \mathbf{P}\mathbf{E}_{\text{out}}\mathbf{P}^\top) = f(\mathbf{P}\mathbf{X}_{\text{in}}, \mathbf{P}\mathbf{E}_{\text{in}}\mathbf{P}^\top, \mathbf{P}\mathbf{A}\mathbf{P}^\top)$ for an arbitrary permutation matrix $\mathbf{P}$.

N2. Effective Communication – The model should facilitate long-range communication between nodes. Numerous real-world tasks require the GNN to capture interactions between distant nodes (Dwivedi et al., 2022). However, MPNN layers, which propagate information locally, frequently fail in this regard (Ma et al., 2023). A major challenge is underreaching, where an MPNN with l layers is incapable of supporting communication between two nodes x_i, x_j with distance $\delta(x_i, x_j) > l$ (Alon and Yahav, 2020). Another challenge is oversquashing, where the structure of the graph forces information from a large set of nodes to squeeze through a small set of nodes to reach its target (Topping et al., 2021). A node with a constant-size feature vector may need to relay information from exponentially many nodes (with respect to model depth), leading to excessive compression of messages in deep MPNNs (Alon and Yahav, 2020).

N3. Selective Aggregation – The model should only aggregate information from relevant nodes and edges. MPNN layers commonly update node representations by unconditionally summing or averaging messages from neighboring nodes and edges (Veličković, 2023). In deep models, this can lead to oversmoothing, where the representation of nodes becomes too similar to be effectively classified in the process of repeated aggregation (Chen et al., 2020). To address this issue, nodes should aggregate information from relevant neighbors only, instead of doing it unconditionally, in order to maintain distinguishability of node representations when necessary.

E1. Relationship Representation – The model should effectively represent the relationships between nodes with edges. Edges in graph-structured data often convey meaningful information about the relationship between the nodes they connect (Gong and Cheng, 2019). In addition to the semantic relationship represented by edge features of the input graph, structural relationship can be represented by edge encodings added by the model (Rampášek et al., 2022). To capture the relationships between nodes, edge representations should combine information from both edge features and encodings, and undergo deep processing through multiple layers.

E2. Directionality Preservation – The model should preserve and utilize information carried by edge directions. Many graphs representing real-world relationships are inherently directed (Rossi et al., 2024). Although edge directionality has been shown to carry important information for various tasks, many GNN variants require undirected graphs as input, to prevent edge directions from restricting information flow (Rossi et al., 2024). It would be beneficial for the model's expressivity if edge directionality information could be preserved without severely limiting communication.

The Structure of GRASS. The high-level structure of GRASS is illustrated in Figure 1. Prior to training, GRASS precomputes the (D-)RRWP encoding of each graph in the dataset. At each training iteration, GRASS randomly rewires the input graph, applies node and edge encodings, and passes the graph through multiple attention layers, producing an output graph with the same structure. For tasks that require graph-level representation, such as graph regression and graph classification, pooling is performed on the output graph to obtain a single output vector.

3.1 GRAPH ENCODING

Extracting structural information plays an important role in graph-structured learning and is crucial for *Relationship Representation*. To this end, we apply relative random walk probabilities (RRWP) encoding (Ma et al., 2023) to represent structural relationships. In addition, we propose D-RRWP, a decomposed variant of RRWP that offers improved computational efficiency.

RRWP Encoding. RRWP encoding has been shown to be an expressive representation of graph structure both theoretically and practically (Ma et al., 2023), serving as a major source of structural information for the model. To calculate random walk probabilities, we first obtain the transition matrix $\mathbf{T}$, where $\mathbf{T}_{i,j}$ represents the probability of moving from node i to node j in a random walk step. It is defined as $\mathbf{T} = \mathbf{D}^{-1}\mathbf{A} : [0,1]^{|V|\times|V|}$, where $\mathbf{A} \in \{0,1\}^{|V|\times|V|}$ is the adjacency matrix of the input graph G, and $\mathbf{D} \in \mathbb{N}^{|V|\times|V|}$ is its degree matrix. The powers of $\mathbf{T}$ are stacked to form the RRWP tensor $\mathbf{P}$, with $\mathbf{P}_{h,i,j}$ representing the probability that a random walker who starts at node i lands at node j at the h-th step. Formally, $\mathbf{P} = [\mathbf{T}, \mathbf{T}^2, ..., \mathbf{T}^k] : [0,1]^{k\times|V|\times|V|}$, where k is the number of random walk steps. The diagonal elements $\mathbf{P}_{:,i,i}$ where $i \in V_G$ are used as node encodings, similarly to RWSE (Dwivedi et al., 2021). The rest are used as edge encodings when the corresponding edge is present in the rewired graph H. All node encodings undergo batch normalization (BN) (Ioffe and Szegedy, 2015) to improve their distribution. Here, $\mathbf{W}$ denotes trainable weights, n denotes the dimensionality of hidden layers, and $\|$ denotes concatenation.

$$\mathbf{x}_i^{\text{RW}} = \mathbf{W}_{\text{node-enc}}\text{BN}(\mathbf{P}_{:,i,i}) : \mathbb{R}^n \tag{1}$$

$$\mathbf{e}_{i,j}^{\text{RW}} = \mathbf{W}_{\text{edge-enc}}\text{BN}(\mathbf{P}_{:,i,j} \,\|\, \mathbf{P}_{:,j,i}) : \mathbb{R}^n \tag{2}$$

Before entering attention layers, RRWP encodings are added to both node features and edge features, including those of edges added by random rewiring. The node encodings are additionally accompanied by degree information (Ying et al., 2021). Here, $\text{d}^+(i)$ and $\text{d}^-(i)$ denote the out-degree and in-degree of node i, respectively.

$$\mathbf{x}_i^0 = \mathbf{x}_i^{\text{in}} + \mathbf{x}_i^{\text{RW}} + \mathbf{W}_{\text{deg}}\text{BN}(\text{d}^+(i) \,\|\, \text{d}^-(i)) : \mathbb{R}^n \tag{3}$$

$$\mathbf{e}_{i,j}^0 = \mathbf{e}_{i,j}^{\text{in}} + \mathbf{e}_{i,j}^{\text{RW}} : \mathbb{R}^n \tag{4}$$

Improving Efficiency. RRWP encodings take $O(k|V||E|)$ time to compute and $O(k|V|^2)$ space to store (Ma et al., 2023). On extremely large graphs, this could be computationally prohibitive even when computed once per dataset. We propose D-RRWP, a decomposed variant of RRWP. Instead of computing the exact random walk probabilities $\mathbf{P}$ form the transition matrix $\mathbf{T}$, we approximate it with its truncated eigendecomposition to reduce the complexity to $O(km(|V| + |E|))$ time and $O((k+m)|V|+k|E|)$ space, where $m \leq |V|$ is the number of eigenpairs used for the approximation.

To ensure that the transition matrix is diagonalizable, we replace $\mathbf{T}$ with $\mathbf{T}_{\text{sym}} = \mathbf{D}^{-\frac{1}{2}}\mathbf{A}\mathbf{D}^{-\frac{1}{2}}$, which is always diagonalizable if $\mathbf{A}$ is a symmetric adjacency matrix—that of an undirected graph. Given the degree matrix $\mathbf{D}$, this modification does not result in a loss of information, because $\mathbf{T}_{\text{sym}} = \mathbf{D}^{\frac{1}{2}}\mathbf{T}\mathbf{D}^{-\frac{1}{2}}$. Since $\mathbf{T}_{\text{sym}}$ is diagonalizable, its truncated eigendecomposition coincides with its truncated singular value decomposition (SVD), which is the *optimal* low-rank approximation of a matrix (Eckart and Young, 1936).

Let $\tilde{\mathbf{T}}_{\text{sym}} = \tilde{\mathbf{Q}}\tilde{\mathbf{\Lambda}}\tilde{\mathbf{Q}}^\top$ be the truncated eigendecomposition of $\mathbf{T}$, where $\tilde{\mathbf{Q}} : [-1,1]^{|V|\times m}$ and $\tilde{\mathbf{\Lambda}} : [-1,1]^{m\times m}$ contain the m-largest (in magnitude) eigenvectors and eigenvalues of $\mathbf{T}_{\text{sym}}$, respectively. Calculating the truncated eigendecomposition of $\mathbf{T}_{\text{sym}}$ takes $O(m|E|)$ time with the Lanczos algorithm (Lanczos, 1950; Lehoucq et al., 1998), and the results can be stored in $O(m|V|)$ space. We approximate $\mathbf{P}_{h,i,j} = \mathbf{T}^h_{\text{sym}\,i,j}$ with $\tilde{\mathbf{T}}^h_{\text{sym}\,i,j} = (\tilde{\mathbf{Q}}\tilde{\mathbf{\Lambda}}^h\tilde{\mathbf{Q}}^\top)_{i,j} = (\tilde{\mathbf{Q}}_i \odot \tilde{\mathbf{Q}}_j) \cdot \tilde{\mathbf{\Lambda}}^h$ which takes $O(km(|V| + |E|))$ time and $O(k(|V| + |E|))$ space to calculate for all nodes, edges, and random walk steps $1 \leq h \leq k$. Here, $\odot$ denotes the Hadamard product. This is possible because we can calculate $\tilde{\mathbf{T}}^h_{\text{sym}}$ by taking the powers of $\tilde{\mathbf{\Lambda}}$, a diagonal matrix, in $O(km)$ time and space. If we were to replace $\mathbf{T}^h_{\text{sym}}$ with a non-diagonalizable transition matrix, and its eigendecomposition with SVD, it would no longer be possible to efficiently calculate its powers.

Since $\tilde{\mathbf{\Lambda}}^h$ can take at most m linearly independent values as we vary h, increasing k beyond m does not add additional information to the encoding. Consequently, we fix $k = m$ in our experiments.

3.2 RANDOM REWIRING

To achieve *Effective Communication*, GRASS rewires the input graph by superimposing a random regular graph. We present some motivations for using random regular graphs instead of deterministic or non-regular graphs in Appendix A.1. Shirzad et al. (2023) uses a similar technique in generalizing BigBird (Zaheer et al., 2020) to graphs, and discusses additional motivations. We also demonstrate the advantage of using random regular graphs with empirical results shown in Figure 4, Table 3 and Table 5. Here, we provide details on random regular graph generation and input graph rewiring.

Generating Random Regular Graphs. We generate random regular graphs with the Permutation Model (Puder, 2015) that we describe here and with pseudocode in Appendix A.2. For a given positive and even parameter $r \geq 2$, and for the input graph $G = (V_G, E_G)$, we randomly generate a corresponding r-regular graph by independently and uniformly sampling $\frac{r}{2}$ random permutations $\sigma_1, \sigma_2, ..., \sigma_{\frac{r}{2}}$ from $S_{|V_G|}$, the symmetric group defined over the nodes of the graph G. Using these random permutations, we construct a random pseudograph $\tilde{R} = (V_G, E_{\tilde{R}})$, where the edge set $E_{\tilde{R}}$ of the graph $\tilde{R}$ is

$$E_{\tilde{R}} = \bigsqcup_{i \in V_G, j \in [\frac{r}{2}]} \{\{i, \sigma_j(i)\}\} \tag{5}$$

Here, $\sqcup$ denotes the disjoint union of sets. The resulting graph $\tilde{R}$ is a random regular pseudograph, and the probability that $\tilde{R}$ is any regular pseudograph with $|V_G|$ nodes and degree r is equal (Bollobás and Fernandez de la Vega, 1982). Being a pseudograph, $\tilde{R}$ might not be simple—it might contain self-loops and multi-edges. Even when $|V_G|$ is large, the probability that $\tilde{R}$ is simple—that it does not contain self-loops or multi-edges—would not be prohibitively small. In particular, it has an asymptotically tight lower bound (Bollobás and Fernandez de la Vega, 1982):

$$\lim_{|V_G| \to \infty} \Pr[\tilde{R} \text{ is simple}] = e^{-\frac{r^2}{2} - r} \tag{6}$$

Therefore, if we re-generate $\tilde{R}$ when it's not simple, the expected number of trials required for us to obtain a simple $\tilde{R}$ is upper-bounded by $e^{\frac{r^2}{2} + r}$, which can be kept low by keeping r low. In practice, GRASS would like the superimposed graph to be simple, in order to avoid passing duplicate messages. Meanwhile, the regularity of the graph is desired but not strictly required. Therefore, when $\tilde{R}$ is not simple, we remove self-loops and multi-edges from $\tilde{R}$ to obtain R, which is always simple but not necessarily regular.

Our empirical results presented in Figure 4, Table 3 and Table 5 suggest that a small value of r is often sufficient. In our experiments, we use $r \leq 6$.

Rewiring the Input Graph. To rewire the input graph G, GRASS superimposes the edges of R on G, producing a new graph $H = (V_G, E_G \sqcup E_R)$ that is used as input for subsequent stages of the model. Since it is possible that $E_G \cap E_R \neq \varnothing$, there might be multi-edges in H, and in these cases, H is not a simple graph. GRASS does not remove these multi-edges to avoid biasing the distribution of the superimposed random regular graph.

The added edges E_R are given a distinct embedding to make them distinguishable from the existing edges E_G. This aids *Selective Aggregation*, as it allows a node to select between its neighbors and a random node. Edge encodings are also given to the added edges, which are instrumental in *Relationship Representation*. Although an added edge $(i, j) \in E_R$ lacks edge features that represent semantic relationships in the input graph, the structural relationship between nodes i and j is represented by the random walk probabilities $\mathbf{P}_{:,i,j}$ given to that edge as its (D-)RRWP encoding.

3.3 ATTENTION MECHANISM

Many GTs emulate the structure of Transformers designed for Euclidean data (Dwivedi and Bresson, 2020; Kreuzer et al., 2021; Ying et al., 2021; Hussain et al., 2022; Shirzad et al., 2023). Meanwhile, GRASS uses attentive node aggregators with attention scores computed by MLP edge aggregators, which is a more tailored attention mechanism for graph-structured data. Figure 3 provides a simple visualization, and Figure 5 illustrates its structure in detail. The GRASS attention mechanism is

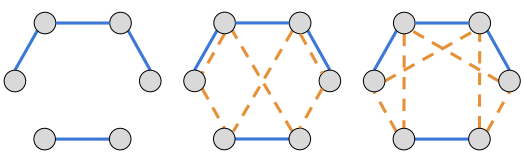

(a) (b) (c)

Figure 2: Visualization of the proposed random rewiring mechanism. Solid lines denote existing edges of the input graph, and dashed lines denote added edges. **(a)** An example of the input graph G that has poor connectivity. **(b, c)** Two among all possible instances of the randomly rewired graph H with $r = 2$. They have better connectivity than the input graph.

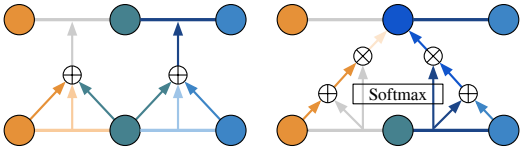

(a) (b)

Figure 3: Simplfied visualization of the proposed attention mechanism. **(a)** The edge aggregator extracting node relations to update edges representations. **(b)** The attentive node aggregator weighted by edge representations. For simplicity, attention from a node to itself, residual connections, and activation functions are omitted here. Figure 5 provides a more detailed visualization.

defined as follows, where $\mathcal{N}^-$ denotes in-neighbors, $\mathbf{W}$ denotes trainable weights, and ε denotes a small constant added for numerical stability. For simplicity, biases are not shown in these equations.

$$\mathbf{s}_{i,j}^l = \text{dropout}\left(\exp(\mathbf{W}_{\text{attn}\leftarrow\text{edge}}^l \mathbf{e}_{i,j}^{l-1})\right) : \mathbb{R}^{+n} \tag{7}$$

$$\mathbf{a}_{i,j}^l = \frac{\mathbf{s}_{i,j}^l}{\sum_{h\in\mathcal{N}^-(j)\cup\{j\}} \mathbf{s}_{h,j}^l + \varepsilon} : \mathbb{R}^{+n} \tag{8}$$

$$\tilde{\mathbf{x}}_j^l = \mathbf{W}_{\text{tail}\leftarrow\text{tail}}^l \mathbf{x}_j^{l-1} + \sum_{i\in\mathcal{N}^-(j)\cup\{j\}} \mathbf{a}_{i,j}^l \odot (\mathbf{W}_{\text{tail}\leftarrow\text{head}}^l \mathbf{x}_i^{l-1} + \mathbf{W}_{\text{tail}\leftarrow\text{edge}}^l \mathbf{e}_{i,j}^{l-1}) : \mathbb{R}^n \tag{9}$$

$$\tilde{\mathbf{e}}_{i,j}^l = \mathbf{W}_{\text{edge}\leftarrow\text{edge}}^l \mathbf{e}_{i,j}^{l-1} + \mathbf{W}_{\text{edge}\leftarrow\text{head}}^l \mathbf{x}_i^{l-1} + \mathbf{W}_{\text{edge}\leftarrow\text{tail}}^l \mathbf{x}_j^{l-1} : \mathbb{R}^n \tag{10}$$

Attention Weights. This attention mechanism is unique in the way it uses edge representations as the medium of attention weights. To satisfy the needs of *Relationship Representation*, edge representations must be updated alongside node representations. Unlike a node, whose neighborhood is a set of nodes, a directed edge always has one head and one tail which is an ordered pair. An undirected edge can be represented by two directed edges with opposite directions, which allows us to generalize this observation to undirected graphs. With an ordered input, an edge can use an MLP as its aggregator while preserving *Permutation Equivariance*. Assuming that *Relationship Representation* is satisfied, edge features would already represent node relationships, which we can use as attention weights $\mathbf{a}_{i,j}$ after applying a linear layer and taking element-wise softmax.

Random Edge Removal. To complement the proposed random rewiring technique, which adds edges but never removes them, GRASS attention randomly removes edges in computing attention weights (Equation 7). The goal is to reduce the model's dependence on the presence of particular edges in the graph, facilitating *Selective Aggregation*. Notably, it can also be seen as a generalization of DropKey (Li et al., 2022) to graphs, because it randomly masks the attention matrix prior to the softmax operation.

Edge Flipping. While the proposed attention mechanism naturally achieves *Directionality Preservation* by aggregating information in the same direction as edges, it can severely restrict the flow of information, putting it in conflict with *Effective Communication*. As a solution, the direction of each edge is switched from one layer to the next: in odd-numbered layers, the directions match those of the edges in the rewired graph H, whereas in even-numbered layers, they are reversed. This enables the model to propagate information in both directions even when the input graph is directed, improving its expressivity.

Feed-Forward Network. Similar to Transformers, the output of the attention mechanism is passed through an FFN. Here, ϕ denotes a ReLU-like (Nair and Hinton, 2010; Ramachandran et al., 2017) nonlinear activation function, which we choose to be Mish (Misra, 2019).

$$\hat{\mathbf{x}}_i^l = \mathbf{W}_{\text{node-out}}^l \phi(\tilde{\mathbf{x}}_i^l + \mathbf{b}_{\text{node-act}}^l) + \mathbf{b}_{\text{node-out}}^l : \mathbb{R}^n \tag{11}$$

$$\hat{\mathbf{e}}_{j,i}^l = \mathbf{W}_{\text{edge-out}}^l \phi(\tilde{\mathbf{e}}_{i,j}^l + \mathbf{b}_{\text{edge-act}}^l) + \mathbf{b}_{\text{edge-out}}^l : \mathbb{R}^n \tag{12}$$

Table 1: Performance on GNN Benchmark Datasets. The performance of GRASS shown here is the mean ± s.d. of 16 runs on ZINC, and 8 runs on other datasets. The **best** and **second-best** results are highlighted. Performance numbers other than that of GRASS are adapted from Ma et al. (2023), Shirzad et al. (2023), and Chen et al. (2024).

Model	ZINC MAE ↓	MNIST Accuracy ↑	CIFAR10 Accuracy ↑	PATTERN Accuracy ↑	CLUSTER Accuracy ↑
GCN	0.367 ± 0.011	90.705 ± 0.218	55.710 ± 0.381	71.892 ± 0.334	68.498 ± 0.976
GIN	0.526 ± 0.051	96.485 ± 0.252	55.255 ± 1.527	85.387 ± 0.136	64.716 ± 1.553
GAT	0.384 ± 0.007	95.535 ± 0.205	64.223 ± 0.455	78.271 ± 0.186	70.587 ± 0.447
GatedGCN	0.282 ± 0.015	97.340 ± 0.143	67.312 ± 0.311	85.568 ± 0.088	73.840 ± 0.326
GatedGCN-LSPE	0.090 ± 0.001	-	-	-	-
PNA	0.188 ± 0.004	97.94 ± 0.12	70.35 ± 0.63	-	-
DGN	0.168 ± 0.003	-	72.838 ± 0.417	86.680 ± 0.034	-
GSN	0.101 ± 0.010	-	-	-	-
CIN	0.079 ± 0.006	-	-	-	-
CRaW1	0.085 ± 0.004	97.944 ± 0.050	69.013 ± 0.259	-	-
GIN-AK+	0.080 ± 0.001	-	72.19 ± 0.13	86.850 ± 0.057	-
SAN	0.139 ± 0.006	-	-	-	76.691 ± 0.65
Graphormer	0.122 ± 0.006	-	-	-	-
K-Subgraph SAT	0.094 ± 0.008	-	-	86.848 ± 0.037	77.856 ± 0.104
EGT	0.108 ± 0.009	98.173 ± 0.087	68.702 ± 0.409	86.821 ± 0.020	79.232 ± 0.348
Graphormer-URPE	0.086 ± 0.007	-	-	-	-
Graphormer-GD	0.081 ± 0.009	-	-	-	-
GPS	0.070 ± 0.004	-	72.298 ± 0.356	86.685 ± 0.059	78.016 ± 0.180
Exphormer	-	98.55 ± 0.039	74.69 ± 0.125	86.74 ± 0.015	78.07 ± 0.037
GRIT	**0.059 ± 0.002**	98.108 ± 0.111	76.468 ± 0.881	**87.196 ± 0.076**	**80.026 ± 0.277**
NeuralWalker	0.065 ± 0.001	**98.760 ± 0.079**	**80.027 ± 0.185**	86.977 ± 0.012	78.189 ± 0.188
GRASS (ours)	**0.047 ± 0.001**	**98.932 ± 0.076**	**83.750 ± 0.141**	**89.177 ± 0.313**	**79.541 ± 0.173**

Normalization and Residual Connection. We use post-normalization in residual connections, which has been shown to improve the expressiveness of Transformers (Liu et al., 2020). The residual connection is scaled by the constant α to improve training stability (Wang et al., 2022).

$$\mathbf{x}_i^l = \mathrm{BN}(\mathbf{x}_i^{l-1} + \alpha\hat{\mathbf{x}}_i^l) : \mathbb{R}^n \tag{13}$$

$$\mathbf{e}_{i,j}^l = \mathrm{BN}(\mathbf{e}_{i,j}^{l-1} + \alpha\hat{\mathbf{e}}_{j,i}^l) : \mathbb{R}^n \tag{14}$$

Graph Pooling. For graph-level tasks, graph pooling is required at the output of a GNN to produce a vector representation of each graph, capturing global properties relevant to the task (Wu et al., 2020). GRASS employs sum pooling, a simple pooling method as powerful as the Weisfeiler-Lehman graph isomorphism test (Leman and Weisfeiler, 1968), while many more complicated methods are not (Baek et al., 2021). Considering the randomness of the added edges, they are pooled separately from the preexisting edges in the input graph G, because the pooled output of the randomly added edges may exhibit a different distribution than that of the preexisting edges. Here, $\|$ denotes concatenation.

$$\mathbf{y} = \sum_{i \in V_G} \mathbf{x}_i^L \,\Big\|\, \sum_{(i,j) \in E_G} \mathbf{e}_{i,j}^L \,\Big\|\, \sum_{(i,j) \in E_R} \mathbf{e}_{i,j}^L \;: \mathbb{R}^{3n} \tag{15}$$

3.4 Interpretations of GRASS

A Message Passing Perspective. GRASS is an MPNN on a noisy graph. In an MPNN, information is propagated along the edges of the input graph, defined by its adjacency matrix (Veličković, 2023). GRASS can be seen as an MPNN that injects additive and multiplicative noise into the adjacency matrix, through random rewiring and random edge removal, respectively. The adjacency matrix $\mathbf{A}_M$ followed by message passing is given by

$$\mathbf{A}_M = (\mathbf{A}_G + \mathbf{A}_R) \cdot \mathbf{A}_D \tag{16}$$

where $\mathbf{A}_G$ is the adjacency matrix of the input graph G, $\mathbf{A}_R$ is that of the superimposed random regular graph R, $\mathbf{A}_D$ is a random attention mask sampled by the dropout function in Equation 7 (which can also be seen as the adjacency matrix of a random graph), $+$ denotes element-wise OR, and $\cdot$ denotes element-wise AND. Noise injection is well known as an effective regularizer (Noh et al., 2017), and for graph-structured data, the random removal of edges has demonstrated regularization effects (Rong et al., 2019).

Table 2: Performance on LRGB datasets. The performance of GRASS shown here is the mean ± s.d. of 8 runs. The **best** and **second-best** results are highlighted. Performance numbers other than that of GRASS are adapted from Gutteridge et al. (2023), Tönshoff et al. (2023), Ma et al. (2023), Shirzad et al. (2023), and Chen et al. (2024). *Tönshoff et al. (2023) has improved the performance of these models via hyperparameter tuning.

Model	Peptides-func AP ↑	Peptides-struct MAE ↓	PascalVOC-SP Macro F1 ↑	COCO-SP Macro F1 ↑
GCN*	0.6860 ± 0.0050	**0.2460 ± 0.0007**	0.2078 ± 0.0031	0.1338 ± 0.0007
GINE*	0.6621 ± 0.0067	0.2473 ± 0.0017	0.2718 ± 0.0054	0.2125 ± 0.0009
GatedGCN*	0.6765 ± 0.0047	0.2477 ± 0.0009	0.3880 ± 0.0040	0.2922 ± 0.0018
DIGL+MPNN	0.6469 ± 0.0019	0.3173 ± 0.0007	0.2824 ± 0.0039	-
DIGL+MPNN+LapPE	0.6830 ± 0.0026	0.2616 ± 0.0018	0.2921 ± 0.0038	-
MixHop-GCN	0.6592 ± 0.0036	0.2921 ± 0.0023	0.2506 ± 0.0133	-
MixHop-GCN+LapPE	0.6843 ± 0.0049	0.2614 ± 0.0023	0.2218 ± 0.0174	-
DRew-GCN	0.6996 ± 0.0076	0.2781 ± 0.0028	0.1848 ± 0.0107	-
DRew-GCN+LapPE	**0.7150 ± 0.0044**	0.2536 ± 0.0015	0.1851 ± 0.0092	-
DRew-GIN	0.6940 ± 0.0074	0.2799 ± 0.0016	0.2719 ± 0.0043	-
DRew-GIN+LapPE	**0.7126 ± 0.0045**	0.2606 ± 0.0014	0.2692 ± 0.0059	-
DRew-GatedGCN	0.6733 ± 0.0094	0.2699 ± 0.0018	0.3214 ± 0.0021	-
DRew-GatedGCN+LapPE	0.6977 ± 0.0026	0.2539 ± 0.0007	0.3314 ± 0.0024	-
Transformer+LapPE	0.6326 ± 0.0126	0.2529 ± 0.0016	0.2694 ± 0.0098	0.2618 ± 0.0031
SAN+LapPE	0.6384 ± 0.0121	0.2683 ± 0.0043	0.3230 ± 0.0039	0.2592 ± 0.0158
GPS+LapPE*	0.6534 ± 0.0091	0.2509 ± 0.0014	0.4440 ± 0.0065	0.3884 ± 0.0055
Exphormer	0.6527 ± 0.0043	0.2481 ± 0.0007	0.3975 ± 0.0037	0.3455 ± 0.0009
GRIT	0.6988 ± 0.0082	**0.2460 ± 0.0012**	-	-
NeuralWalker	0.7096 ± 0.0078	0.2463 ± 0.0005	**0.4912 ± 0.0042**	**0.4398 ± 0.0033**
GRASS (ours)	0.6737 ± 0.0064	**0.2459 ± 0.0007**	**0.5670 ± 0.0049**	**0.4752 ± 0.0032**

A Graph Transformer Perspective. GRASS is a sparse Graph Transformer. Graph Transformers allow each node to aggregate information from other nodes through graph attention mechanisms, with a general definition (Veličković, 2023) being

$$\mathbf{x}'_j = \phi\left(\mathbf{x}_j, \bigoplus_{i \in \mathcal{N}(j)} a(\mathbf{x}_i, \mathbf{x}_j)\psi(\mathbf{x}_i)\right) \tag{17}$$

where ϕ and ψ are neural networks, a is an attention weight function, and $\bigoplus$ is a permutation-invariant aggregator. Many GTs compute attention weights using scaled dot-product attention (Vaswani et al., 2017), with node features as keys and queries. However, we observe that edge features in GRASS, which are updated by aggregating information from its head and tail nodes with an MLP, could be used to directly compute attention weights as a form of additive attention (Bahdanau et al., 2014). *Relationship Representation* would then be critical for the attention weights to be meaningful, which GRASS satisfies through expressive edge encodings and the deep processing of edge features. Many GTs achieve sparsity by integrating (Rampášek et al., 2022) or generalizing (Shirzad et al., 2023) BigBird's sparse dot-product attention. Meanwhile, GRASS achieves sparsity in a graph-native way: attention is always local, so non-adjacent nodes in the rewired graph would naturally never attend to each other. Seeing GRASS as a Transformer, its attention mask would be $\mathbf{A}_M$ as defined in Equation 16, which contains $O(r|V| + |E|)$ nonzero elements.

4 Experiments

4.1 Benchmarking GRASS

Experimental Setup. To measure the performance of GRASS, we train and evaluate it on five of the GNN Benchmark Datasets (Dwivedi et al., 2023): ZINC, MNIST, CIFAR10, CLUSTER, and PATTERN, as well as four of the Long Range Graph Benchmark (LRGB) (Dwivedi et al., 2022) datasets: Peptides-func, Peptides-struct, PascalVOC-SP, and COCO-SP. Following the experimental setup of Rampášek et al. (2022) and other work that we compare, we configure GRASS to around 100k parameters for MNIST and CIFAR10, and 500k parameters for all other datasets. Additional information on the datasets can be found in Appendix E.1.

Due to the use of random rewiring, the output of the model is not deterministic. Therefore, we evaluate the trained model 100 times for ZINC, and 10 times for other datasets, for each training run. The average performance is reported as the performance of that run. We use D-RRWP encoding

Table 3: Ablation study results for the number of added edges per node, with random regular and non-regular graphs, on ZINC. Reported values, except peak VRAM consumption, are the mean ± s.d. over 8 runs. The variance of model performance due to random rewiring are measured by evaluating the test set 100 times on each trained model. For comparison, the variance of model performance due to randomness in the training process is 1.79e-6.

# Added Edge per Node		0	3	6	9	12	Fully Connected
MAE ↓	Regular	0.0557 ± 0.0021	0.0480 ± 0.0019	0.0470 ± 0.0013	0.0484 ± 0.0018	0.0483 ± 0.0012	0.0492 ± 0.0008
	Non-Regular		0.0488 ± 0.0015	0.0486 ± 0.0020	0.0480 ± 0.0019	0.0475 ± 0.0021	
Variance in MAE Due to Random Rewiring	Regular	Deterministic	7.60e-8 ± 3.67e-8	1.37e-7 ± 1.00e-7	1.67e-7 ± 8.51e-8	2.24e-7 ± 1.11e-7	Deterministic
	Non-Regular		1.20e-7 ± 9.23e-8	1.39e-7 ± 4.75e-8	1.63e-7 ± 1.19e-7	9.94e-8 ± 4.47e-8	
Training Time per Epoch (s)	Regular	1.74 ± 0.02	1.81 ± 0.10	1.95 ± 0.07	2.02 ± 0.05	2.19 ± 0.05	2.40 ± 0.03
	Non-Regular		1.75 ± 0.04	1.87 ± 0.07	2.00 ± 0.03	2.20 ± 0.04	
Peak VRAM Consumption (MiB)	Regular	1415	1911	2529	3051	3569	4273
	Non-Regular		1889	2489	3009	3511	

on Peptides-func, PascalVOC-SP and COCO-SP, and RRWP encoding on other datasets. Models are trained with the Lion optimizer (Chen et al., 2023). Hyperparameters can be found in Appendix E.2.

Results. As shown in Tables 1 and 2, GRASS ranks first on ZINC, MNIST, CIFAR, PATTERN, Peptides-struct, PascalVOC-SP, and COCO-SP, while ranking second on CLUSTER and fifth on Peptides-func, among the models compared. Notably, GRASS achieves 20.3% lower MAE in ZINC compared to GRIT (Ma et al., 2023), the second-best model, which has $O(|V|^2)$ time and space complexity.

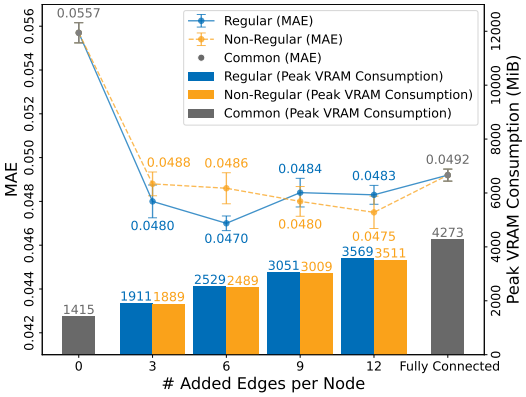

Figure 4: Visualized ablation study results for the number of added edges per node, with random regular and non-regular graphs, on ZINC. Error bars represent one standard deviation. The setup is identical to that described in Table 3.

4.2 Ablation Study

Experimental Setup. We examine the impact of RRWP encoding and D-RRWP encoding by comparing their performance with each other and with LapPE, a popular graph encoding technique. We examine the effects of random rewiring by varying the number of added edges per node, and adding random non-regular graphs instead of random regular graphs. Furthermore, we assess the effects of the GRASS attention mechanism by replacing it with the attention mechanisms of GAT (Veličković et al., 2017), GatedGCN (Bresson and Laurent, 2017), and Transformer (Vaswani et al., 2017), while keeping the rest of the model intact. These experiments are conducted on ZINC, a well-known GNN benchmark that represents tasks on smaller graphs, and PascalVOC-SP, which represents tasks on larger graphs that require long-range interaction, with detailed results for the latter presented in Appendix C. Additionally on ZINC, we explore the impact of minor design choices including random edge removal, edge flipping, normalization, graph pooling, and the optimizer. The findings suggest that the combination of (D-)RRWP, random rewiring, and GRASS attention demonstrates superior effectiveness compared to alternative combinations on the evaluated datasets.

Random Walk Encoding. On both ZINC and PascalVOC-SP, switching between RRWP and D-RRWP results in an insignificant change in performance: 0.64% on ZINC and 0.35% on PascalVOC-SP. However, replacing D-RRWP with RRWP results in a 17.73× larger preprocessed dataset on PascalVOC-SP. This highlights the viability of D-RRWP as an efficient replacement of RRWP on larger graphs. Replacing RRWP or D-RRWP with LapPE results in a significant degradation of performance on ZINC, but a much smaller degradation on PascalVOC-SP, indicating that the combination of LapPE with other components of GRASS are not as effective and more dataset-dependent.

Table 4: Ablation study results for graph encoding, attention mechanism, and minor design decisions on ZINC. This table shows the performance of each ablated model as the mean ± s.d. over 8 runs. The implementations of replacement attention mechanisms are provided by PyTorch Geometric (Fey and Lenssen, 2019), and we adjust the head size to approach 500k parameters. *The maximum number of Laplacian eigenvectors to use for LapPE on ZINC is 8, which is constrained by the smallest graph in the dataset. For a fair comparison, we include a setup that pads the LapPE of smaller graphs with zeros to raise the maximum number of eigenvectors to 32. †The learning rate is adjusted for these configurations to stabilize training. ‡The batch size, learning rate, betas, and weight decay factor are adjusted for this configuration to stabilize training.

Setup	MAE ↓
GRASS	0.0470 ± 0.0013
RRWP (32 steps) → D-RRWP (32 eigenpairs, 32 steps)	0.0473 ± 0.0021
RRWP (32 steps) → LapPE (8 eigenvectors)*	0.0829 ± 0.0041
RRWP (32 steps) → Padded LapPE (32 eigenvectors)*	0.0879 ± 0.0067
GRASS attention → GAT attention (Veličković et al., 2017)	0.0592 ± 0.0023
GRASS attention → GatedGCN attention† (Bresson and Laurent, 2017)	0.0651 ± 0.0030
GRASS attention → Transformer attention† (Vaswani et al., 2017)	0.0652 ± 0.0016
No random edge removal	0.0500 ± 0.0018
No edge flipping	0.0470 ± 0.0010
BN → LN (Ba et al., 2016)	0.0497 ± 0.0009
Sum pooling → Mean pooling	0.0493 ± 0.0024
Lion → AdamW‡ (Loshchilov et al., 2017)	0.0499 ± 0.0006

Random Rewiring. On both ZINC and PascalVOC-SP, the optimal number of added edges per node is 6 with random regular graphs, while adding more or fewer edges leads to suboptimal performance. On ZINC, switching from regular to non-regular random graphs increases the number of added edges required to achieve similar performance, resulting in longer runtime and higher memory consumption. This demonstrates the advantage of random rewiring with regular graphs.

GRASS Attention. On both ZINC and PascalVOC-SP, replacing GRASS attention with alternative attention mechanisms substantially degrades performance, by at least 26.0% on ZINC and 14.7% on PascalVOC-SP. This indicates that GRASS attention, our novel design, is a vital component for GRASS to achieve competitive performance.

Minor Design Decisions. None of the minor design decisions, when altered or removed, results in a significant performance degradation on ZINC: an advantage of at least 15.2% is maintained compared to GRIT, the second-best model. This verifies that the performance advantage of GRASS is achieved mainly by the proposed combination of encoding, rewiring, and attention mechanism.

5 Conclusion

We have presented GRASS, a novel GNN architecture that synergistically integrates (D-)RRWP encoding, random rewiring, and a new graph-tailored additive attention mechanism. Our empirical evaluations show that GRASS achieves and often surpasses state-of-the-art performance across a diverse set of benchmark problems.

5.1 Limitations

Evaluation of Scalability. GRASS has $O(|V| + |E|)$ time and space complexity, which implies good scalability to extremely large-and-sparse graphs. We regret to say that evaluating GRASS thoroughly on these datasets is not currently within the scope of this project, due to time and resource constraints. We aim to further explore the scalability of GRASS in future work.

Nondeterministic Output. The output of GRASS is inherently random due to random rewiring. The relationship between performance variance and the number of randomly added edges is demonstrated in Table 3 and Table 5. In scenarios that strictly require deterministic output, the random number generator used for random rewiring needs to be seeded with the input graph, making the deployment of GRASS more complicated in these scenarios.

5.2 Reproducibility Statement

The source code of GRASS is available here: https://anonymous.4open.science/r/grass.

References

Uri Alon and Eran Yahav. On the bottleneck of graph neural networks and its practical implications. *arXiv preprint arXiv:2006.05205*, 2020.

Adrian Arnaiz-Rodriguez, Ahmed Begga, Francisco Escolano, and Nuria Oliver. Diffwire: Inductive graph rewiring via the lovasz bound. In *The First Learning on Graphs Conference*, 2022.

Jimmy Lei Ba, Jamie Ryan Kiros, and Geoffrey E Hinton. Layer normalization. *arXiv preprint arXiv:1607.06450*, 2016.

Jinheon Baek, Minki Kang, and Sung Ju Hwang. Accurate learning of graph representations with graph multiset pooling. *arXiv preprint arXiv:2102.11533*, 2021.

Dzmitry Bahdanau, Kyunghyun Cho, and Yoshua Bengio. Neural machine translation by jointly learning to align and translate. *arXiv preprint arXiv:1409.0473*, 2014.

Mitchell Black, Zhengchao Wan, Amir Nayyeri, and Yusu Wang. Understanding oversquashing in gnns through the lens of effective resistance. In *International Conference on Machine Learning*, pages 2528–2547. PMLR, 2023.

Béla Bollobás and W Fernandez de la Vega. The diameter of random regular graphs. *Combinatorica*, 2:125–134, 1982.

Xavier Bresson and Thomas Laurent. Residual gated graph convnets. *arXiv preprint arXiv:1711.07553*, 2017.

Deli Chen, Yankai Lin, Wei Li, Peng Li, Jie Zhou, and Xu Sun. Measuring and relieving the over-smoothing problem for graph neural networks from the topological view. In *Proceedings of the AAAI conference on artificial intelligence*, volume 34, pages 3438–3445, 2020.

Dexiong Chen, Till Hendrik Schulz, and Karsten Borgwardt. Learning long range dependencies on graphs via random walks. *arXiv preprint arXiv:2406.03386*, 2024.

Xiangning Chen, Chen Liang, Da Huang, Esteban Real, Kaiyuan Wang, Yao Liu, Hieu Pham, Xuanyi Dong, Thang Luong, Cho-Jui Hsieh, et al. Symbolic discovery of optimization algorithms. *arXiv preprint arXiv:2302.06675*, 2023.

Vijay Prakash Dwivedi and Xavier Bresson. A generalization of transformer networks to graphs. *arXiv preprint arXiv:2012.09699*, 2020.

Vijay Prakash Dwivedi, Anh Tuan Luu, Thomas Laurent, Yoshua Bengio, and Xavier Bresson. Graph neural networks with learnable structural and positional representations. *arXiv preprint arXiv:2110.07875*, 2021.

Vijay Prakash Dwivedi, Ladislav Rampášek, Michael Galkin, Ali Parviz, Guy Wolf, Anh Tuan Luu, and Dominique Beaini. Long range graph benchmark. *Advances in Neural Information Processing Systems*, 35:22326–22340, 2022.

Vijay Prakash Dwivedi, Chaitanya K Joshi, Anh Tuan Luu, Thomas Laurent, Yoshua Bengio, and Xavier Bresson. Benchmarking graph neural networks. *Journal of Machine Learning Research*, 24(43):1–48, 2023.

Carl Eckart and Gale Young. The approximation of one matrix by another of lower rank. *Psychometrika*, 1(3):211–218, 1936.

Wendy Ellens, Floske M Spieksma, Piet Van Mieghem, Almerima Jamakovic, and Robert E Kooij. Effective graph resistance. *Linear algebra and its applications*, 435(10):2491–2506, 2011.

David Ellis. The expansion of random regular graphs. *Lecture Notes, Lent*, 34, 2011.

Matthias Fey and Jan Eric Lenssen. Fast graph representation learning with pytorch geometric. *arXiv preprint arXiv:1903.02428*, 2019.

Liyu Gong and Qiang Cheng. Exploiting edge features for graph neural networks. In *Proceedings of the IEEE/CVF conference on computer vision and pattern recognition*, pages 9211–9219, 2019.

Frank Göring. Short proof of menger's theorem. *Discrete Mathematics*, 219(1-3):295–296, 2000.

Benjamin Gutteridge, Xiaowen Dong, Michael M Bronstein, and Francesco Di Giovanni. Drew: Dynamically rewired message passing with delay. In *International Conference on Machine Learning*, pages 12252–12267. PMLR, 2023.

Will Hamilton, Zhitao Ying, and Jure Leskovec. Inductive representation learning on large graphs. *Advances in neural information processing systems*, 30, 2017.

Md Shamim Hussain, Mohammed J Zaki, and Dharmashankar Subramanian. Global self-attention as a replacement for graph convolution. In *Proceedings of the 28th ACM SIGKDD Conference on Knowledge Discovery and Data Mining*, pages 655–665, 2022.

Sergey Ioffe and Christian Szegedy. Batch normalization: Accelerating deep network training by reducing internal covariate shift. In *International conference on machine learning*, pages 448–456. pmlr, 2015.

Kedar Karhadkar, Pradeep Kr Banerjee, and Guido Montúfar. Fosr: First-order spectral rewiring for addressing oversquashing in gnns. *arXiv preprint arXiv:2210.11790*, 2022.

Thomas N Kipf and Max Welling. Semi-supervised classification with graph convolutional networks. *arXiv preprint arXiv:1609.02907*, 2016.

Devin Kreuzer, Dominique Beaini, Will Hamilton, Vincent Létourneau, and Prudencio Tossou. Rethinking graph transformers with spectral attention. *Advances in Neural Information Processing Systems*, 34:21618–21629, 2021.

Cornelius Lanczos. An iteration method for the solution of the eigenvalue problem of linear differential and integral operators. 1950.

Richard B Lehoucq, Danny C Sorensen, and Chao Yang. *ARPACK users' guide: solution of large-scale eigenvalue problems with implicitly restarted Arnoldi methods*. SIAM, 1998.

AA Leman and Boris Weisfeiler. A reduction of a graph to a canonical form and an algebra arising during this reduction. *Nauchno-Technicheskaya Informatsiya*, 2(9):12–16, 1968.

Bonan Li, Yinhan Hu, Xuecheng Nie, Congying Han, Xiangjian Jiang, Tiande Guo, and Luoqi Liu. Dropkey. *arXiv preprint arXiv:2208.02646*, 2022.

Liyuan Liu, Xiaodong Liu, Jianfeng Gao, Weizhu Chen, and Jiawei Han. Understanding the difficulty of training transformers. *arXiv preprint arXiv:2004.08249*, 2020.

Ilya Loshchilov, Frank Hutter, et al. Fixing weight decay regularization in adam. *arXiv preprint arXiv:1711.05101*, 5, 2017.

JF Lutzeyer and AT Walden. Comparing graph spectra of adjacency and laplacian matrices. *arXiv preprint arXiv:1712.03769*, 2017.

Liheng Ma, Chen Lin, Derek Lim, Adriana Romero-Soriano, Puneet K Dokania, Mark Coates, Philip Torr, and Ser-Nam Lim. Graph inductive biases in transformers without message passing. *arXiv preprint arXiv:2305.17589*, 2023.

Diganta Misra. Mish: A self regularized non-monotonic activation function. *arXiv preprint arXiv:1908.08681*, 2019.

Vinod Nair and Geoffrey E Hinton. Rectified linear units improve restricted boltzmann machines. In *Proceedings of the 27th international conference on machine learning (ICML-10)*, pages 807–814, 2010.

Hyeonwoo Noh, Tackgeun You, Jonghwan Mun, and Bohyung Han. Regularizing deep neural networks by noise: Its interpretation and optimization. *Advances in neural information processing systems*, 30, 2017.

Doron Puder. Expansion of random graphs: New proofs, new results. *Inventiones mathematicae*, 201(3):845–908, 2015.

Prajit Ramachandran, Barret Zoph, and Quoc V Le. Searching for activation functions. *arXiv preprint arXiv:1710.05941*, 2017.

Ladislav Rampášek, Michael Galkin, Vijay Prakash Dwivedi, Anh Tuan Luu, Guy Wolf, and Dominique Beaini. Recipe for a general, powerful, scalable graph transformer. *Advances in Neural Information Processing Systems*, 35:14501–14515, 2022.

Yu Rong, Wenbing Huang, Tingyang Xu, and Junzhou Huang. Dropedge: Towards deep graph convolutional networks on node classification. *arXiv preprint arXiv:1907.10903*, 2019.

Emanuele Rossi, Bertrand Charpentier, Francesco Di Giovanni, Fabrizio Frasca, Stephan Günnemann, and Michael M Bronstein. Edge directionality improves learning on heterophilic graphs. In *Learning on Graphs Conference*, pages 25–1. PMLR, 2024.

Hamed Shirzad, Ameya Velingker, Balaji Venkatachalam, Danica J Sutherland, and Ali Kemal Sinop. Exphormer: Sparse transformers for graphs. In *International Conference on Machine Learning*, pages 31613–31632. PMLR, 2023.

Jan Tönshoff, Martin Ritzert, Eran Rosenbluth, and Martin Grohe. Where did the gap go? reassessing the long-range graph benchmark. *arXiv preprint arXiv:2309.00367*, 2023.

Jake Topping, Francesco Di Giovanni, Benjamin Paul Chamberlain, Xiaowen Dong, and Michael M Bronstein. Understanding over-squashing and bottlenecks on graphs via curvature. *arXiv preprint arXiv:2111.14522*, 2021.

Ashish Vaswani, Noam Shazeer, Niki Parmar, Jakob Uszkoreit, Llion Jones, Aidan N Gomez, Łukasz Kaiser, and Illia Polosukhin. Attention is all you need. *Advances in neural information processing systems*, 30, 2017.

Petar Veličković. Everything is connected: Graph neural networks. *Current Opinion in Structural Biology*, 79:102538, 2023.

Petar Veličković, Guillem Cucurull, Arantxa Casanova, Adriana Romero, Pietro Lio, and Yoshua Bengio. Graph attention networks. *arXiv preprint arXiv:1710.10903*, 2017.

Hongyu Wang, Shuming Ma, Li Dong, Shaohan Huang, Dongdong Zhang, and Furu Wei. Deepnet: Scaling transformers to 1,000 layers. *arXiv preprint arXiv:2203.00555*, 2022.

Zonghan Wu, Shirui Pan, Fengwen Chen, Guodong Long, Chengqi Zhang, and S Yu Philip. A comprehensive survey on graph neural networks. *IEEE transactions on neural networks and learning systems*, 32(1):4–24, 2020.

Keyulu Xu, Weihua Hu, Jure Leskovec, and Stefanie Jegelka. How powerful are graph neural networks? *arXiv preprint arXiv:1810.00826*, 2018.

Chengxuan Ying, Tianle Cai, Shengjie Luo, Shuxin Zheng, Guolin Ke, Di He, Yanming Shen, and Tie-Yan Liu. Do transformers really perform badly for graph representation? *Advances in Neural Information Processing Systems*, 34:28877–28888, 2021.

Seongjun Yun, Minbyul Jeong, Raehyun Kim, Jaewoo Kang, and Hyunwoo J Kim. Graph transformer networks. *Advances in neural information processing systems*, 32, 2019.

Manzil Zaheer, Guru Guruganesh, Kumar Avinava Dubey, Joshua Ainslie, Chris Alberti, Santiago Ontanon, Philip Pham, Anirudh Ravula, Qifan Wang, Li Yang, et al. Big bird: Transformers for longer sequences. *Advances in neural information processing systems*, 33:17283–17297, 2020.

A Random Rewiring

A.1 Motivations for Superimposing Random Regular Graphs

Effects on Diameter. The diameter of a graph upper-bounds the distance between two nodes, and thus the number of layers for an MPNN to propagate information between them (Alon and Yahav, 2020). Superimposing a random regular graph onto the input graph can drastically decrease its diameter. The least integer d that satisfies

$$(r-1)^{d-1} \geq (2+\varepsilon)r|V|\log|V| \tag{18}$$

is the upper bound of the diameter of almost every random r-regular graph with $|V|$ nodes, where $r \geq 3$ and $\varepsilon > 0$ (Bollobás and Fernandez de la Vega, 1982). Since adding edges to a graph never increases its diameter, the diameter d of the rewired graph is asymptotically upper-bounded by $d \in O(\log_r |V|)$ when $r \geq 3$. Subsequently, all nodes would be able to communicate with each other given $O(\log_r |V|)$ message passing layers, which could significantly reduce the risk of underreaching on large graphs. In addition, the diameter of a graph is a trivial upper bound of its effective resistance (Ellens et al., 2011), which has been shown to be positively associated with oversquashing (Black et al., 2023). Intuitively, it upper bounds the "length" of the bottleneck through which messages are passed.

Effects on Internally Disjoint Paths. Since oversquashing can be attributed to squeezing too many messages through the fixed-size feature vector of a node (Alon and Yahav, 2020), increasing the number of internally disjoint paths between two nodes may reduce oversquashing by allowing information to propagate through more nodes in parallel. Intuitively, it increases the "width" of the bottleneck. A random r-regular graph with $r \geq 2$ almost certainly has a vertex connectivity of r as $|V| \to \infty$ (Ellis, 2011). Menger's Theorem then lower-bounds the number of internally disjoint paths by a graph's vertex connectivity (Göring, 2000).

Effects on Spectral Gap. Oversquashing has been shown to decrease as the spectral gap of a graph increases, which is defined as λ_1, the smallest positive eigenvalue of the graph's Laplacian matrix (Karhadkar et al., 2022). It has been proven that a random r-regular graph sampled uniformly from the set of all r-regular graphs with $|V|$ nodes almost certainly has $\mu < 2\sqrt{r-1}+1$ as $|V| \to \infty$, where μ is the largest absolute value of nontrivial eigenvalues of its adjacency matrix (Puder, 2015). Since the graph is r-regular, its i-th adjacency matrix eigenvalue μ_i and i-th Laplacian matrix eigenvalue λ_i satisfy $\lambda_i = r - \mu_i$ (Lutzeyer and Walden, 2017), lower-bounding the spectral gap with $\lambda_1 > r - 2\sqrt{r-1} - 1$.

A.2 Pseudocode of the Permutation Model

Algorithm 1 The Permutation Model (Puder, 2015)

procedure PermutationModel(r, $|V|$)
  $\sigma \leftarrow$ 2D array of size $(r, |V|)$
  for $i \leftarrow 0$ to $r-1$ **do**
    $\sigma[i,:] \leftarrow$ RandPerm($|V|$) ▷ Random permutation of integers between 0 and $|V|-1$
  end for
  $A \leftarrow$ Array of size $r \times |V|$ ▷ Create an empty adjacency list
  for $j \leftarrow 0$ to $|V|$ **do**
    for $k \leftarrow 0$ to r **do**
      $A[j \times r + k] \leftarrow \{j, \sigma[k,j]\}$ ▷ Add an edge to the adjacency list
    end for
  end for
  $A \leftarrow$ RemoveSelfLoop(A) ▷ Remove self-loops from the adjacency list
  $A \leftarrow$ RemoveMultiEdge(A) ▷ Remove multi-edges from the adjacency list
  return A
end procedure

B GRASS ATTENTION

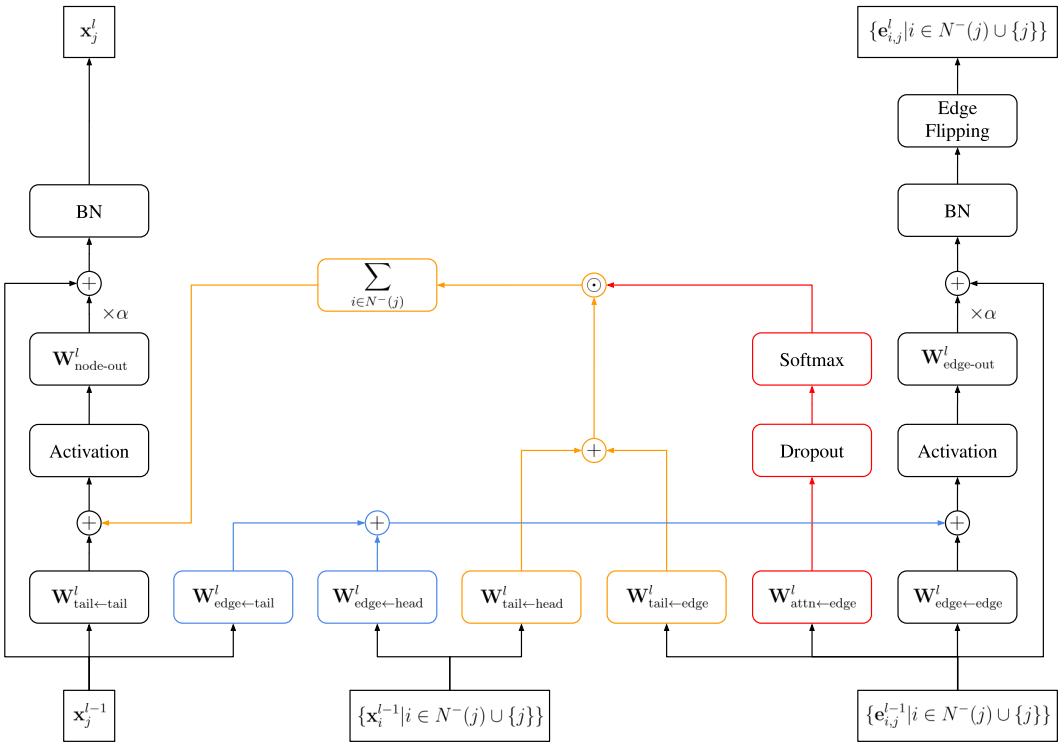

Figure 5: The structure of an attention layer of GRASS. Node aggregation is attentive, with attention weights derived from edge representations. Edge aggregation is done through an MLP. For simplicity, biases are not shown here.

C Additional Ablation Studies

Table 5: Ablation study results for the number of added edges per node, with random regular and non-regular graphs, on PascalVOC-SP. Reported values, except peak VRAM consumption, are the mean ± s.d. over 8 runs. The experimental setup is identical to that described in Table 3. For comparison, the variance of model performance due to randomness in the training process is 2.36e-5.

# Added Edge per Node	0	3	6	9	12
Macro F1 ↑	0.4430 ± 0.0105	0.5606 ± 0.0102	0.5670 ± 0.0049	0.5612 ± 0.0056	0.5619 ± 0.0075
Variance in Macro F1 Due to Random Rewiring	Deterministic	3.40e-6 ± 2.12e-6	2.86e-6 ± 8.51e-7	2.27e-6 ± 9.32e-7	2.54e-6 ± 1.37e-6
Training Time per Epoch (s)	15.66 ± 0.07	29.55 ± 0.16	42.96 ± 0.09	56.31 ± 0.16	69.87 ± 0.28
Peak VRAM (MiB)	8525	14191	19893	25591	31231

Table 6: Ablation study results for graph encoding, graph rewiring, and attention mechanism on PascalVOC-SP. This table shows the performance of each ablated model as the mean ± s.d. over 4 runs. The experimental setup is identical to that described in Table 4. *Using RRWP encoding with 128 random walk steps would result in OOM during preprocessing. With D-RRWP (128 eigenpairs, 128 steps), the preprocessed dataset has size 6.40 GiB, while with RRWP (32 steps), the preprocessed dataset has size 113.46 GiB, which is 17.73× larger.

Setup	Macro F1 ↑
GRASS	0.5670 ± 0.0049
D-RRWP (128 eigenpairs, 128 steps) → RRWP (32 steps)*	0.5690 ± 0.0045
D-RRWP (128 eigenpairs, 128 steps) → LapPE (128 eigenvectors)	0.5387 ± 0.0070
Random Regular Rewiring → Random Non-Regular Rewiring	0.5622 ± 0.0081
GRASS attention → GAT attention (Veličković et al., 2017)	0.4663 ± 0.0079
GRASS attention → GatedGCN attention† (Bresson and Laurent, 2017)	0.4414 ± 0.0075
GRASS attention → Transformer attention† (Vaswani et al., 2017)	0.4835 ± 0.0062

D Computational Performance

Table 7: Computational performance of GRASS on GNN Benchmark Datasets. Training time per epoch is the wall-clock time taken to complete a single training epoch, shown as the mean ± s.d. over 30 epochs. Preprocessing time is the wall-clock time taken to load, preprocess, and store the whole dataset prior to training. Specifications of the hardware used to run these experiments are also shown here.

Dataset	ZINC	MNIST	CIFAR10	PATTERN	CLUSTER
Training Time per Epoch (s)	1.87 ± 0.07	11.83 ± 0.21	15.56 ± 0.10	33.58 ± 0.05	25.34 ± 0.03
Preprocessing Time	25s	1m 1s	1m 32s	33s	27s
Model Compilation	Yes				
Activation Checkpointing	No				
CPU	AMD Ryzen 9 9950X				
GPU	NVIDIA RTX A6000 Ada				

Table 8: Computational performance of GRASS on LRGB datasets. Training time per epoch is shown as the mean ± s.d. over 30 epochs for Peptides-func and Peptides-struct, and over 10 epochs for PascalVOC-SP and COCO-SP. The definition of statistics are identical to that described in Table 7.

Dataset	Peptides-func	Peptides-struct	PascalVOC-SP	COCO-SP
Training Time per Epoch (s)	6.19 ± 0.30	5.90 ± 0.03	42.96 ± 0.09	539.50 ± 0.32
Preprocessing Time	1m 10s	1m 32s	3m 58s	19m 49s
Model Compilation	Yes			Yes
Activation Checkpointing	No			Yes
CPU	AMD Ryzen 9 9950X			
GPU	NVIDIA RTX A6000 Ada			

E EXPERIMENTAL SETUP

E.1 DATASETS

Table 9: Statistics of GNN Benchmark Datasets used in section 4, adapted from Rampášek et al. (2022).

Dataset	# Graphs	Avg. # Nodes	Avg. # Edges	Directionality	Task	Metric
ZINC	12000	23.2	24.9	Undirected	Graph Regression	MAE ↓
MNIST	70000	70.6	564.5	Directed	Graph Classif.	Accuracy ↑
CIFAR10	60000	117.6	941.1	Directed	Graph Classif.	Accuracy ↑
PATTERN	14000	118.9	3039.3	Undirected	Node Classif.	Accuracy ↑
CLUSTER	12000	117.2	2150.9	Undirected	Node Classif.	Accuracy ↑

Table 10: Statistics of LRGB datasets used in section 4, adapted from Dwivedi et al. (2022).

Dataset	# Graphs	Avg. # Nodes	Avg. # Edges	Avg. Short. Path	Avg. Diameter	Task	Metric
Peptides-func	15535	150.94	307.30	20.89 ± 9.79	56.99 ± 28.72	Graph Classif.	AP ↑
Peptides-struct	15535	150.94	307.30	20.89 ± 9.79	56.99 ± 28.72	Graph Regression	MAE ↓
PascalVOC-SP	11355	479.40	2710.48	10.74 ± 0.51	27.62 ± 2.13	Node Classif.	Macro F1 ↑
COCO-SP	123286	476.88	2693.67	10.66 ± 0.55	27.39 ± 2.14	Node Classif.	Macro F1 ↑

E.2 HYPERPARAMETERS

Table 11: Model hyperparameters for experiments on GNN Benchmark Datasets. Experimental results are shown in table 1.

Model	ZINC	MNIST	CIFAR10	PATTERN	CLUSTER
# Parameters	496545	103690	103738	495298	495558
# Attention Layers	49	15	15	53	53
Attention Layer Dim.	32	24	24	32	32
Task Head Hidden Dim.	192	144	144	N/A (Linear)	N/A (Linear)
# Epochs	2000	200	400	500	50
Warmup Epoch Ratio	0.1	0.05	0.1	0.1	0.1
Batch Size	200	200	200	200	200
Initial Learning Rate	1e-7	1e-7	1e-7	1e-7	1e-7
Peak Learning Rate	5e-4	1e-3	1e-3	1e-3	1e-3
Final Learning Rate	1e-7	1e-7	1e-7	3e-4	1e-7
Betas	(0.95, 0.98)	(0.95, 0.98)	(0.95, 0.98)	(0.95, 0.98)	(0.95, 0.98)
Weight Decay Factor	0.5	0.3	0.3	3.0	0.3
Label Smoothing Factor	N/A (Regression)	0.1	0.1	0.1	0.1
Random Walk Encoding Type	RRWP	RRWP	RRWP	RRWP	RRWP
(D-)RRWP Random Walk Length	32	24	24	32	32
Random Regular Graph Degree	6	6	6	6	6
Random Edge Removal Rate	0.1	0.1	0.1	0.5	0.5

Table 12: Model hyperparameters for experiments on LRGB datasets. Experimental results are shown in table 2.

Model	Peptides-func	Peptides-struct	PascalVOC-SP	COCO-SP
# Parameters	500074	498315	501493	499377
# Attention Layers	48	48	53	53
Attention Layer Dim.	32	32	32	32
Task Head Hidden Dim.	192	192	N/A (Linear)	N/A (Linear)
# Epochs	500	500	500	100
Warmup Epoch Ratio	0.1	0.1	0.1	0.1
Batch Size	200	200	200	200
Initial Learning Rate	1e-7	1e-7	1e-7	1e-7
Peak Learning Rate	1e-3	1e-3	1e-3	1e-3
Final Learning Rate	1e-7	1e-7	1e-7	1e-7
Betas	(0.95, 0.98)	(0.95, 0.98)	(0.95, 0.98)	(0.95, 0.98)
Weight Decay Factor	0.3	3.0	1.0	0.3
Label Smoothing Factor	0.1	N/A (Regression)	0.1	0.1
Random Walk Encoding Type	D-RRWP	RRWP	D-RRWP	D-RRWP
(D-)RRWP Random Walk Length	128	64	128	64
Random Regular Graph Degree	3	3	6	6
Random Edge Removal Rate	0.1	0.1	0.1	0.1